

# Real-time trace-level detection of carbon dioxide and ethylene in car exhaust gases

Michael T. McCulloch, Nigel Langford, and Geoffrey Duxbury

A direct-absorption spectrometer, based on a pulsed, distributed feedback, quantum cascade laser with a 10.26- $\mu\text{m}$  wavelength and an astigmatic Herriott cell with a 66-m path length, has been developed for high-resolution IR spectroscopy. This spectrometer utilizes the intrapulse method, an example of sweep integration, in which the almost linear wavelength up-chirp obtained from a distributed feedback, quantum cascade laser yields a spectral microwindow of as many as 2.5 wave numbers/ $\text{cm}^{-1}$ . Within this spectral microwindow, molecular fingerprints can be monitored and recorded in real time. This system allows both the detection of carbon dioxide and ethylene and the real-time observation of the evolution of these gases in the exhaust by-products from several cars. © 2005 Optical Society of America

OCIS codes: 120.6200, 300.6260, 300.6340, 300.6390, 010.1120, 280.1740.

## 1. Introduction

Many compact and sensitive mid-IR spectrometers have been constructed with lead-salt lasers, carbon dioxide lasers, or difference frequency mixing (DFM) schemes<sup>1–3</sup> as the light source. Fried *et al.*<sup>1</sup> built a lead-salt, laser-based system for the detection of formaldehyde. Richter *et al.*<sup>2</sup> constructed several different DFM systems that have been used to detect a range of atmospheric pollutants, in particular formaldehyde. Nagele and Sigrist<sup>3</sup> showed that optoacoustic spectrometers based on a carbon dioxide laser can be used to make sensitive measurements of both ethylene and ammonia at ground level. While these approaches have allowed effective spectrometers with trace-level sensitivity there are several disadvantages with each method. Lead-salt lasers produce low-output powers and require cryogenic cooling. DFM schemes require mixing the outputs of two lasers in a nonlinear crystal. In addition, to obtain the desired output wavelength, the frequency produced by each laser must be well defined, which adds to the complexity of a system. The output powers of a DFM system are typically submilliwatt. Carbon dioxide la-

asers can generate significant output powers; however, the physical size and electrical power consumption can limit their usefulness in portable systems.

A spectrometer, capable of operating at room temperature, that does not face these problems is one based on the quantum cascade (QC) laser. Kosterev and Tittel<sup>4</sup> recently reviewed the performance characteristics of QC-laser-based spectrometers. The QC lasers were operated in both the pulsed and cw mode to as high as room temperature.<sup>4</sup> Continuous-wave lasers, however, are currently commercially available for operation only at 77 K, although significant advances in room-temperature operation have been made by Yarekha *et al.*,<sup>5</sup> Anders *et al.*,<sup>6</sup> and Yu *et al.*<sup>7</sup> The intrasubband transitions in the devices lead to narrow free-running linewidths of 1–3 MHz,<sup>4</sup> operating wavelengths between 3 and 16  $\mu\text{m}$ , and output powers in the 100-mW regime. Webster *et al.*<sup>8</sup> have shown that cryogenically cooled cw QC lasers are useful replacements for lead-salt lasers.

Pulsed QC lasers operating close to room temperature are better sources for many types of spectrometer since they do not require bulky cryogenic cooling systems. Two different ways of using pulsed QC lasers in spectrometers have been developed, the interpulse<sup>9</sup> and the intrapulse methods.<sup>10</sup> The first of these to be developed, by Namjou *et al.*,<sup>9</sup> was the interpulse method. In this approach a short-duration current pulse of approximately 10 ns is applied to the QC laser. The resulting optical output pulse is tuned through an absorption feature by use of a slowly varying subthreshold current ramp. The typical tuning range achieved with this approach is as many as

---

The authors are with the Department of Physics, University of Strathclyde, John Anderson Building, 107 Rottenrow, Glasgow, G4 0NG, United Kingdom. G. Duxbury's e-mail is G.Duxbury@strath.ac.uk.

Received 30 December 2003; revised manuscript received 6 October 2004; accepted 29 October 2004.

0003-6935/05/142887-08\$15.00/0

© 2005 Optical Society of America

0.74 wave numbers/cm<sup>-1</sup>. The intrapulse method was developed subsequently by Normand *et al.*<sup>10</sup> This scheme relies on the almost linear frequency downchirp obtained from a pulsed QC laser to map spectral information into the temporal domain. We have shown recently that such a spectrometer is a sensitive instrument for detecting the absorption of trace gases.<sup>11</sup> In particular we have shown<sup>11</sup> the power of this system for recording the fingerprint spectrum of molecules such as COF<sub>2</sub>, CF<sub>2</sub>CH<sub>2</sub>, CO<sub>2</sub>, and H<sub>2</sub>O within the spectral microwindow defined by the laser chirp. In this paper we demonstrate the potential of the spectrometer for detecting atmospheric pollutants by showing that we can detect trace levels of carbon dioxide and ethylene in real time.

Car exhaust pollution is thought to be the single largest source of many gaseous pollutants in urban areas.<sup>12</sup> In a comprehensive analysis of the sources of low-level ozone production Derwent *et al.*<sup>13</sup> have shown that the gases emitted from motor vehicle exhausts, in particular ethylene, exhibit the highest ozone-forming potential of all the major hydrocarbon emission sources that they evaluated. As a result of this and other comprehensive studies, legislation has been introduced designed to reduce these emissions. To track the efficacy of this legislation, the monitoring of car exhausts has become important. The different gases emitted from a car and their relative concentrations tell us about the health of its engine. Poorly maintained cars, and wear and tear in the engine, may lead to greater emission of carbon monoxide and hydrocarbons.<sup>12</sup> Another important factor is the air/fuel ratio  $\lambda$  of the combustion mixture because this also affects the relative emission of gases. When  $\lambda < 1$  the air/fuel mixture is said to be rich. In this regime, which is most common at engine start-up, the exhaust contains more unburned hydrocarbons and carbon monoxide. When  $\lambda > 1$  the air/fuel mixture is said to be lean. In this regime carbon monoxide and hydrocarbon emissions are low. However, nitrogen oxides are not lowered because there is no reductant such as carbon monoxide or a hydrocarbon. If  $\lambda = 1$ , the emission components are at their minimum and the mixture is stoichiometrical. Cars fitted with catalytic converters,<sup>14,15</sup> designed to reduce harmful emissions, can operate with control of their air/fuel ratio  $\lambda$  control. This allows the air/fuel mixture to be optimized during the running of the engine.

## 2. Experimental Design

Our system has been described in previous work.<sup>10,11</sup> The spectrometer has been modified to allow flow-through experiments to be carried out. The layout is shown in Fig. 1. The QC laser was fabricated by Alpes Lasers to operate at 10.26  $\mu$ m. The QC laser heat sink was mounted on a Peltier cooler in an airtight chamber supplied by Alpes Lasers. The light was coupled out of the chamber through an antireflection-coated ZnSe window. The temperature of the heat

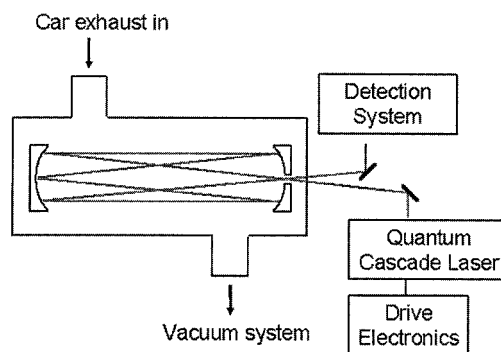


Fig. 1. Schematic diagram of the apparatus. The multipass cell is an astigmatic Herriott cell used with 134 traversals, giving a path length of 66 m.

sink could be varied between  $-40\text{ }^{\circ}\text{C}$  and  $+40\text{ }^{\circ}\text{C}$  with a stability of  $\pm 0.01\text{ }^{\circ}\text{C}$ . The laser was excited by a pulsed current source designed within our group to deliver pulses ranging from 3 ns to 1.5  $\mu$ s at repetition frequencies as great as 100 kHz. The pulsed current source comprises a stabilized digital delay pulse generator (Stanford DG535) that triggers a fast current switcher (DEI HV100), with a jitter of less than 100 ps, that switches the output of a stable current supply designed in our group. This system produces reproducible top-hat-shaped current pulses with a leading edge rise time of  $\sim 2$  ns.

Previous measurements of the behavior of this laser<sup>10,11</sup> indicate a temperature-tuning rate of  $-7.6 \times 10^{-2}\text{ cm}^{-1}/\text{K}$ , corresponding to a frequency downchirp of 2.3 GHz/K. The QC radiation is collected by an off-axis paraboloid and coupled into the gas cell, which contains an astigmatic Herriott mirror arrangement designed to give a 66-m path length. The spot pattern was chosen following the use of a ray-tracing program, written by one of us (M. T. McCulloch), which follows the method of McManus *et al.*<sup>16</sup> The path length was verified by measuring the delay between the trigger pulse and the detector signal.

The input port of the gas cell is connected to the car exhaust by a flexible hosepipe of 50-m length and 15-mm internal diameter. The output port is connected to the vacuum system. A constant pressure of approximately 35 Torr is maintained in the cell as the exhaust gases flow through. The dwell time of the exhaust gases in the cell is controlled by the mass flow through the hosepipe and the pressure differential between the hosepipe and the cell and has been calculated to be approximately 2 s, assuming that all the gas in the cell is exchanged. This is limited primarily by the cell volume and can be reduced by a factor of 10 if a small volume cell is used such as that of Shi *et al.*<sup>17</sup> The input and output ports are located away from the ends of the cell as shown in Fig. 1. This helps to isolate the mirrors from the exhaust gases but produces a nonuniform distribution of the exhaust gas within the volume of the cell defined by the position of the mirrors. The number density mea-

sured in the experiments is therefore the average distribution within the 66-m optical path length.

After leaving the cell, the light is focused onto a fast mercury-cadmium-telluride detector (Kolmar KV104-0.25A). The output from the detector is amplified with a 1.1-GHz bandwidth amplifier (Femto HS-Y-1-40) and recorded with a high-speed (500-MHz bandwidth, 2-G sample) digital signal averager (Aqiris AP200) housed within the control computer.

#### A. Signal Characteristics of the Intrapulse Spectrometer

Some of the characteristics of the spectra produced with the rapid frequency downchirp were described in our previous paper<sup>11</sup> in which the spectra of comparatively heavy molecules such as carbonyl fluoride were studied. We showed that the instrument resolution is set by the time-frequency uncertainty relation<sup>11</sup> and is given by  $\Delta\nu = (Cdv/dt)^{1/2}$ , with  $C$  determined by the temporal profile of the pulse and  $dv/dt$  the chirp rate. For the laser used in this work the chirp rate was 200 MHz/ns, and so, assuming a square temporal pulse profile, the calculated resolution is 421 MHz ( $0.013\text{ cm}^{-1}$ ). This resolution is comparable with that made by Beyer *et al.*<sup>18</sup> on free-running pulsed QC lasers.

Other aspects of the instrument response of the intrapulse spectrometer, however, did not become evident until the spectra of molecules with much less congested spectra, such as ethylene, were examined in detail. Figure 2(a) shows both a high-resolution spectrum of ethylene, obtained by Blake *et al.*,<sup>19</sup> and the same spectrum that has been broadened numerically approximately matching the resolution of the QC spectrometer. The wave-number range shown matches that covered by the QC laser. When the QC laser is used to probe low-pressure samples of ethylene, the resulting instrument response that is obtained resembles that of a swept-frequency, magnetic-resonance spectrometer as shown in Fig. 2(b). Although the resolution is similar to that of the broadened spectrum of Fig. 2(a), the characteristic overshoot, which follows many of the absorption lines, is a signature of rapid passage.

The origin of this rapid-passage behavior has been described in detail by Ernst<sup>20</sup> and occurs when the sweep rate is much faster than the relaxation rate of the medium, which in our case is the time of the collisions between gas molecules. At a low gas pressure of 1–100 m Torr this is approximately 100 times slower than the time taken to sweep through a Doppler-broadened absorption line. In this regime the nonequilibrium transfer of population between the lower and the upper states of the transition may take place, and power saturation can occur as described by Ernst.<sup>20</sup> However, in the presence of a buffer gas such as air the collision frequency may become sufficiently large that rapid passage is suppressed, as is power saturation, and a symmetrical instrument function is obtained. This behavior is shown in Fig. 2(b) as the line shape is modified from

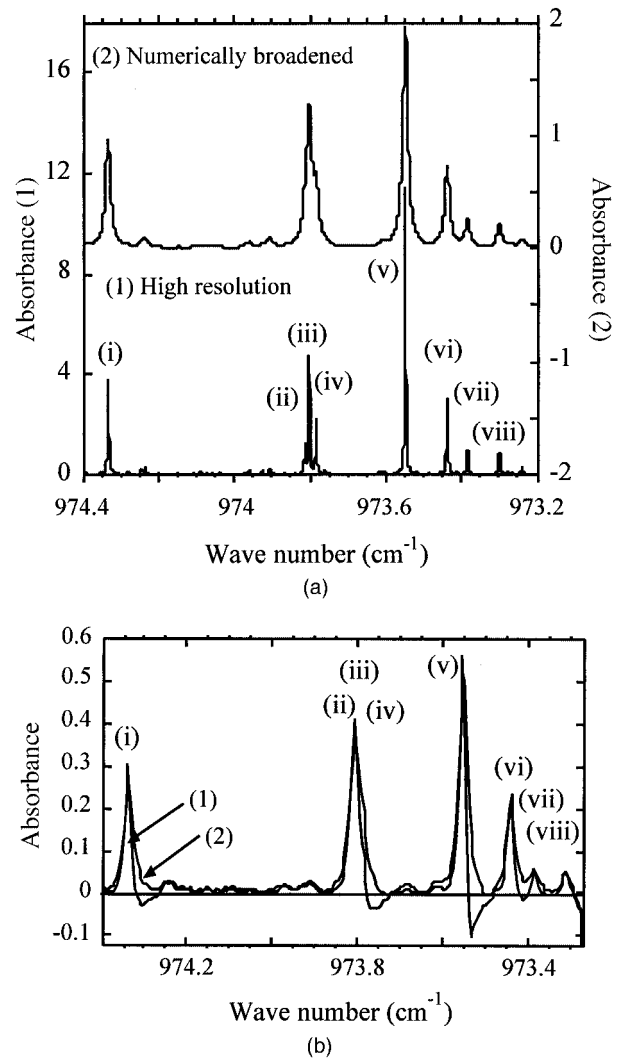


Fig. 2. Comparison of a portion of (a) a high-resolution Fourier-transform spectra of ethylene with (b) the same region recorded with a QC-laser spectrometer. (a) High-resolution absorption spectrum of ethylene recorded by T. A. Blake, R. L. Sams, and S. W. Sharpe in the Environmental Molecular Science Laboratory at Pacific Northwest National Laboratory, Richland, Washington. The gas pressure is 4.98 Torr, and the path length is 15 cm. (1) Absorbance with a maximum resolution of  $0.002\text{ cm}^{-1}$ . The absorption lines are labeled from (i) to (viii), and their assignments are in Table 1. (2) The spectrum broadened to a half-width of  $0.12\text{ cm}^{-1}$  to match the effective resolution of the QC-laser spectrometer. The series of lines, (ii) to (iv), are only partially resolved at this resolution and in the QC-laser spectra. (b) Spectrum of 2.1-mTorr ethylene recorded with the QC-laser spectrometer with a path length of 66 m. (1) Pure gas. (2) Broadened with nitrogen, the total pressure in the cell is 35 Torr. The rapid passage signals, characterized by a rapid transition from absorption to apparent emission when observed at (1) low pressure are quenched when nitrogen is admitted, leading to (2) a conventional pressure broadened line shape at a total pressure in the cell of 35 Torr.

the rapid passage to a conventional form. We described and analyzed these processes recently.<sup>21</sup> The reduced atmospheric pressures at which we chose to operate in the present series of experiments,  $\sim 35$  Torr, are those that eliminate rapid-passage ef-

fects and power saturation while preserving the best resolution possible.

The intrapulse spectrometer operating in a sweep-integration mode exhibits characteristics that are similar to those described recently by Richard *et al.*<sup>22</sup> for fast scan integration. The intrapulse spectrometer acquires a spectrum in a short time compared with environmental fluctuations and electronic drifts. It therefore has similar advantages and sensitivity to their instrument, such as reducing the interference from nonresonant scattering and broad background absorptions, while in addition reducing optical interference fringes within the absorption cell. To demonstrate that our instrument does yield a signal-to-noise ratio for  $N$  averages that is close to the ideal limit of  $N^{1/2}$ , in Fig. 3 we show, using a 110-m path length, an example of noise reduction in part of the 8- $\mu\text{m}$  transmission spectrum of nitrous oxide at a low pressure. The 8- $\mu\text{m}$  QC laser used here has a much slower chirp rate than the 10- $\mu\text{m}$  QC laser, resulting in a resolution of approximately 150 MHz, which has been verified by using the vibration-rotation lines of nitrous oxide. As the number of averages is increased from 2 to 64,000, the largest number of sequential scans that the Aqiris digitizer can process, many more absorption lines may be identified in the spectra as the noise is reduced. The integrated absorbance of the weakest lines detected when 16,000 and 64,000 scans are used, Fig. 3(c), is approximately 500 times less than the strongest lines detected when only 2 scans are used, Fig. 3(a). The upper limit to the sensitivity demonstrated in this way is  $\sim 30$  ppb.

#### B. Measurement and Processing of Experimental Spectra

In the present system at the start of each experiment two reference spectra are recorded. The first of these is the background transmission through the empty cell, and the second is of the etalon reference fringes, with a separation of  $0.0481\text{ cm}^{-1}$ , produced by inserting a short germanium etalon into the laser beam. The exhaust spectra are then recorded sequentially. A number of MATLAB (The Mathworks) routines have been developed within our group to facilitate processing the raw spectra. First, the raw spectra are converted from the time domain to the wave-number domain by using a calibration routine. This routine uses the etalon fringes, of known wave-number separation, to derive a relative wave-number calibration for the sweep. The ethylene and carbon dioxide lines that occur within the spectral tuning range are identified, and a peak fitting routine is then used to determine the relative wave number of each of these lines. Absolute wave-number calibration is then achieved by comparing the relative wave-number calibrated spectrum with the reference spectra of ethylene and carbon dioxide. Each exhaust spectrum is then divided by the background spectrum to produce a succession of transmission spectra. The transmission spectra are converted into absorbance when their natural logarithm is taken. Another routine is used to calculate the partial pressures of the ethylene

and carbon dioxide. The absorption lines are then integrated numerically, and a scaling factor of path length and line intensity is used to yield a partial pressure, which is then used to derive the mixing ratio.

The cars were started from cold and left to idle during the experiment. The calibration of the sensitivity of the instrument for the detection of ethylene was made in two ways, one used the dilution approach and the other relied on the detection of weak lines arising from hot bands or lines having a low transition moment. In the dilution approach, successive dilutions of a known amount of ethylene by dry nitrogen are made. By comparing the two methods, we can show that with the present number of signal averages and the maximum line strength available in our scan region a sensitivity of less than 1.5 ppm of ethylene is achievable for this configuration of the spectrometer.

### 3. Results

In this section we present the data that we obtained by measuring the time dependence of the molecular components of the exhaust gases of a variety of cars belonging to members of the university staff. From these measurements we selected spectra recorded from three of these cars, a Renault Clio, a Honda s2000, and a BMW 318i. These spectra were chosen as examples of the effects of car age and engine capacity on the emission profiles, which vary considerably. All the spectra recorded were an average of 5000 scans. With a repetition rate of 5 kHz we obtained a time resolution of 1 s. The base temperature of the laser was set to 273 K, and the laser was excited by a 5-A, 140-ns-duration, current pulse. This gave a spectral window extending from  $973$  to  $974.4\text{ cm}^{-1}$ . In these conditions the effective spectral resolution was  $\sim 0.014\text{ cm}^{-1}$  as described above. The first car for which we recorded the spectrum of the exhaust gases was a Renault Clio 1.2 16v semiautomatic (2002 model) with a petrol engine.

Part of the spectrum is shown in Fig. 4. In Fig. 4(a) a portion of spectra recorded soon after starting the car is compared with an equivalent spectrum of pressure-broadened ethylene. Within each spectrum two strong ethylene absorption lines and one strong carbon dioxide absorption line are clearly seen. The identities of these lines are in Table 1. The ethylene data in Table 1 are taken from the HITRAN database.<sup>23</sup> These data are in good agreement with those in the ethylene planetary modelers' atlas<sup>24</sup> that was used for cross checking. The line parameters of carbon dioxide given in Table 1 were also taken from the HITRAN database,<sup>23</sup> while those in Table 2 for nitrous oxide were taken from the tables of Maki and Wells.<sup>25</sup> In Fig. 4(b) the spectra of the strongest ethylene line are shown at longer times after the car is switched on. The weak absorption line detectable at 110 s after switch-on corresponds to a concentration of  $\sim 1.5$  ppm. In previous measurements of ethylene concentrations, using a pulsed QC-laser spectrome-

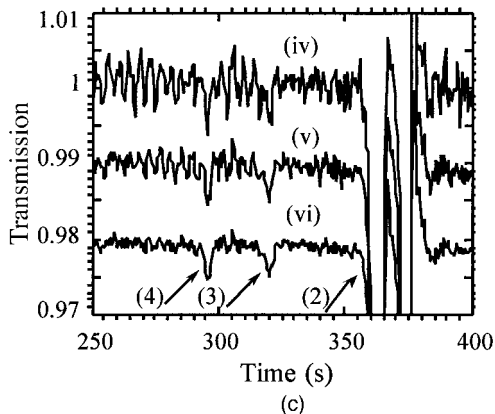
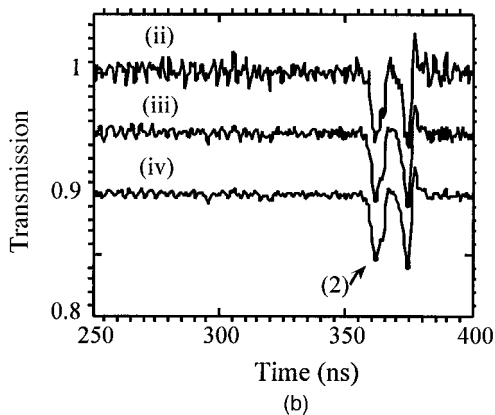
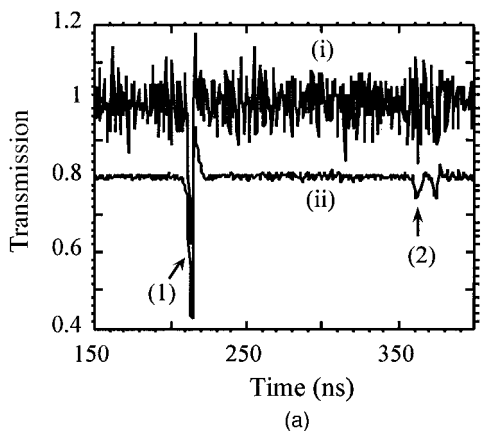


Fig. 3. Portion of the 7.84- $\mu\text{m}$  spectrum of nitrous oxide used to demonstrate the variation of the signal to noise and sensitivity of the spectrometer as a function of the number of averages employed. In an ideal system with  $N$  averages, the signal-to-noise ratio should be improved by  $\sqrt{N}$ . The pressure in the Herriott cell is 0.5 mTorr, and the path length is 110 m. The identification of the absorption lines of nitrous oxide is in Table 2. (a) Spectra recorded by using (i) 2 and (ii) 256 averages; the improvement in the signal to noise is close to that predicted of a factor of 11. Only line (1) can be identified with 2 averages, whereas the closely spaced doublet (2), each line of which is  $\sim 15$  times weaker, may be easily detected in spectrum (ii). (b) Expanded section of the spectrum recorded with (ii) 256, (iii) 1024, and (iv) 4100 averages. The improvement in the signal to noise from (ii) to (iv) is close to the expected value of 4. (c) Greatly expanded section of the spectrum to demonstrate the ability of the spectrometer to clearly detect very weak absorption at the maximum number of averages permitted by the Aqiris digitizer, 64,000. The traces correspond to (iv) 4100, (v) 16,400, and (vi) 64,000. Weak lines (3) and (4) seen in traces (iv)

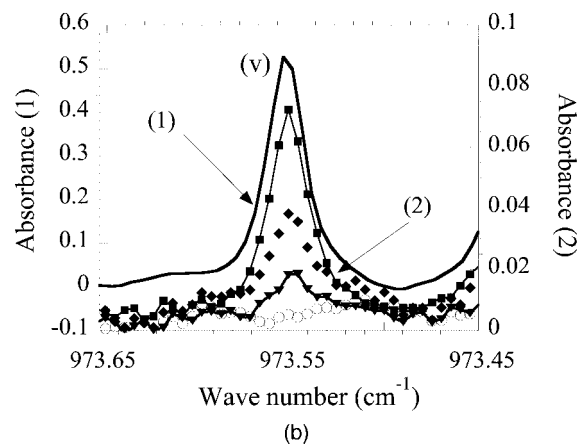
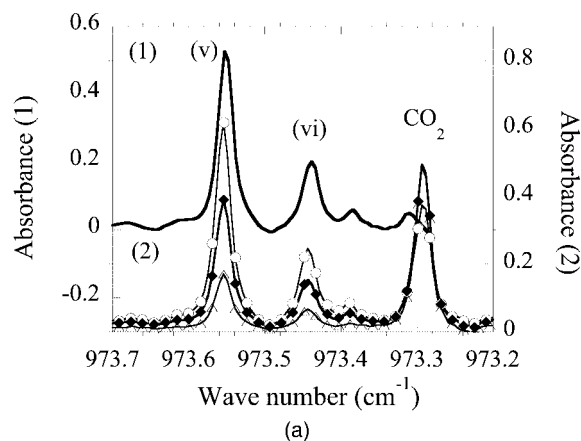


Fig. 4. Comparison of a pressure-broadened spectrum of ethylene and that of the exhaust gas of a Renault Clio car. The identities of the absorption lines are in Table 1. All spectra are recorded at a total cell pressure of  $\sim 35$  Torr. (a) The spectra in the region from 973.7 to 973.2  $\text{cm}^{-1}$  are compared early in the emission process when the ethylene concentration is large and where the concentration of the carbon dioxide in the exhaust region changes slowly. Delay times: open circles, 15 s; solid diagonal square, 40 s; open triangles, 60 s. (b) Spectra of line (v) at longer delay times: solid squares, 80 s; solid diagonal squares, 90 s; solid triangles, 110 s; open circles, 120 s. The weak ethylene absorption seen at 110 s corresponds to a detectivity of  $\sim 1.5$  ppm.

ter, Schilt *et al.*<sup>26</sup> were able to achieve a detectivity of 60 ppm. This limit is in part due to the inability of their spectrometer to resolve closely spaced absorption lines. Since our spectrometer allows us to resolve almost completely the rotational structure within our microwindow, we are able to exploit this resolution to better determine the partial pressure of ethylene in the exhaust gases. This combination of selectivity

and (v) have an intensity approximately 430 times weaker than line 1 and are first seen in trace (v), which has a theoretical signal-to-noise improvement of 90 times spectrum (i) and in trace (vi) where the improvement is 179 times. Since we have shown that this detectivity can be maintained when the total cell pressure is  $\sim 35$ , this leads to an upper limit of detection sensitivity for nitrous oxide with an average of 16,400 scans and a path length of 110 m,  $1.2 \times 10^{-3}$  mTorr in 35-Torr total cell pressure, or 0.03 ppm.

**Table 1. Positions, Assignments, and Intensities of the Vibration–Rotation Transitions of the  $\nu_7$  Band of Ethylene<sup>a,b</sup> and of the  $00^01 - 10^00$  Band of Carbon Dioxide<sup>a</sup> Observed within the Tuning Range of the 10.25- $\mu\text{m}$  QC Laser, 973.2–974.4  $\text{cm}^{-1}$**

Spectra	Wave Number/ $\text{cm}^{-1a,b}$	Integrated Intensity $\text{cm}^{-1}/(\text{molecule}^{-2})^{a,b}$	$J'_{Ka'Kc'}$	$J''_{Ka'Kc'}$	Band	Rotational Transition
Ethylene line label						
(i)	974.33665	$1.152 \times 10^{-20}$	8 <sub>2,6</sub>	7 <sub>1,6</sub>		
(ii)	973.81647	$2.351 \times 10^{-21}$	23 <sub>2,21</sub>	22 <sub>3,19</sub>		
(iii)	973.80553	$1.224 \times 10^{-20}$	15 <sub>3,12</sub>	15 <sub>2,14</sub>		
(iv)	973.78725	$5.095 \times 10^{-21}$	18 <sub>4,15</sub>	18 <sub>3,15</sub>		
(v)	973.55239	$2.355 \times 10^{-20}$	9 <sub>1,8</sub>	8 <sub>0,8</sub>		
(vi)	973.44152	$7.436 \times 10^{-21}$	6 <sub>2,5</sub>	5 <sub>1,5</sub>		
(vii)	973.38790	$1.606 \times 10^{-21}$	7 <sub>5,2</sub>	8 <sub>4,4</sub>		
(viii)	973.30404	$9.815 \times 10^{-22}$	12 <sub>6,7</sub>	13 <sub>5,9</sub>		
CO <sub>2</sub>	973.28852	$2.290 \times 10^{-23}$			00 <sup>0</sup> 1–10 <sup>0</sup> 0	R (16)

<sup>a</sup>Ref. 23.

<sup>b</sup>Ref. 24.

**Table 2. Positions, Assignments, and Intensities of the Vibration–Rotation Transitions of the  $\nu_3$  Band of Nitrous Oxide<sup>a</sup> Observed within the Tuning Range of the 7.84- $\mu\text{m}$  QC Laser, 1277–1274.6  $\text{cm}^{-1}$**

N <sub>2</sub> O Line	Wave Number ( $\text{cm}^{-1}$ )	Integrated Intensity, $\text{cm}^{-1}/(\text{molecule}^{-2})$	Band	Rotational Transition
1	1276.36576	$1.336 \times 10^{-19}$	00 <sup>0</sup> 1–00 <sup>0</sup> 0	P(10)
2	1275.89524	$8.544 \times 10^{-21}$	01 <sup>1</sup> 1–01 <sup>1</sup> 0	P(18) <i>f</i>
2	1275.88774	$8.544 \times 10^{-21}$	01 <sup>1</sup> 1–01 <sup>1</sup> 0	P(18) <i>e</i>
3	1276.01964	$3.80 \times 10^{-22}$	02 <sup>1</sup> 1–02 <sup>2</sup> 0	P(24) <i>f</i>
3	1276.01429	$3.80 \times 10^{-22}$	02 <sup>2</sup> 1–02 <sup>2</sup> 0	P(24) <i>e</i>
4	1276.12731	$3.07 \times 10^{-22}$	00 <sup>2</sup> 1–00 <sup>0</sup> 0	P(5), <sup>14</sup> N <sup>15</sup> N <sup>16</sup> O

<sup>a</sup>Ref. 23.

and sensitivity provided by the frequency downchirp spectrometer is far greater than would have been possible when either the coarse tuning sweep or the photoacoustic method of the earlier experiment is used.<sup>26</sup>

By studying the time dependence of the spectra in Fig. 4, we can see that the largest concentration of ethylene occurs soon after start-up under a cold-start regime. After this period a study of successive spectra reveals that the concentration of ethylene decreases. The concentration of carbon dioxide shows a different

time dependence from that of ethylene. Although its concentration increases in the cold-start period in a way similar to that of ethylene, once it has reached a maximum it decreases to an asymptotic limit as the engine and catalytic converter approach a normal operating temperature.

Figures 5–7 show the time-evolution characteristics of ethylene and carbon dioxide for three different types of petrol engine powered automobile. Figure 5 shows the time evolution of the partial pressures of carbon dioxide and ethylene in the exhaust of a 2002

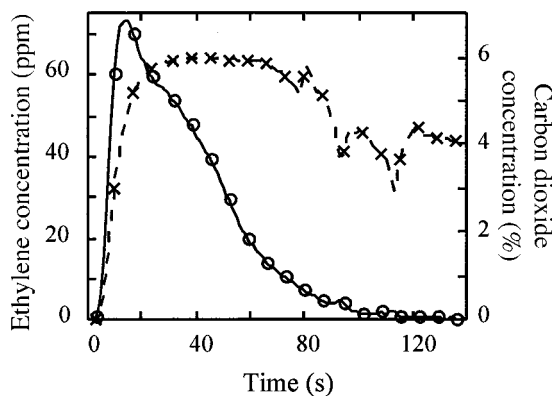


**Fig. 5. Time dependence of the mixing ratios of ethylene and of carbon dioxide in the exhaust gases of a Renault Clio petrol engine. Note the disappearance of ethylene after approximately 110 s.**

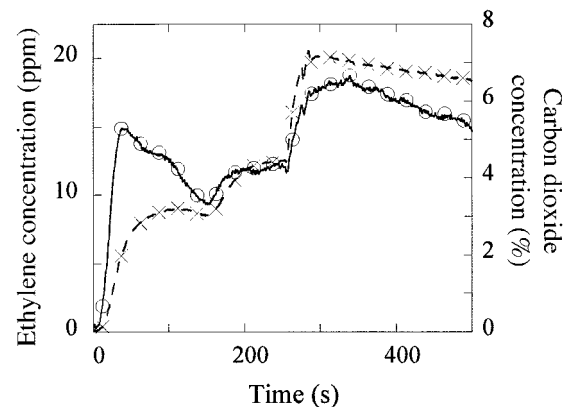


**Fig. 6. Time dependence of the mixing ratios of ethylene and of carbon dioxide in the exhaust gases of a Honda s2000 car. Note that unlike the pattern in the Renault Clio, Fig. 5, high concentrations of ethylene persist at long delay times.**

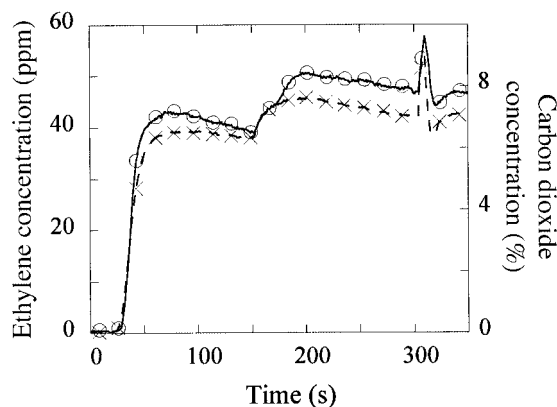


Fig. 7. Time dependence of the mixing ratios of ethylene and of carbon dioxide in the exhaust gases of a BMW 318i car. In contrast with the emissions from the previous cars, the time dependences of the emittance profiles of ethylene and carbon dioxide are almost identical.

semiautomatic Renault Clio from before start-up until after 2 min of running. The spikes in the carbon dioxide and ethylene levels are thought to result from the car's  $\lambda$  control system altering the air/fuel mixture as the engine warms up. This experiment was repeated with a 2000 Honda s2000. Figure 6 shows the time evolution of the partial pressures of carbon dioxide and ethylene in the exhaust from before start-up until after 6 min of running. A BMW 318i automatic car was also tested. Figure 7 shows the time evolution of the partial pressures of carbon dioxide and ethylene in the exhaust from before start-up until after 5 min of running. It can be seen from Figs. 5–7 that the emission patterns of our three test cars are very different. One of the major differences is the persistence of the ethylene in the exhaust gases past the cold-start region for both the BMW and the Honda. Repeating this in traffic conditions would lead to a buildup of ethylene, hence to an enhanced potential for the production of ground level ozone as described by Derwent *et al.*<sup>13</sup>

#### 4. Conclusions

We have demonstrated a simple mid-IR spectrometer that is capable of making sensitive real-time measurements of the concentration of molecular gases, which are important in the study of ground level vehicle pollution. We have also shown that our spectrometer is able to detect multiple species simultaneously with only a single laser. This contrasts with the approach successfully adopted by the Aerodyne group<sup>17,27</sup> in which multiple lasers are used for different narrow microwindows. We have also demonstrated, using the 8- $\mu\text{m}$  spectrum of nitrous oxide as an example, that with appropriate lasers, molecular absorbers, and averaging, sensitivities of 30 ppb may be obtained with the intrapulse method. This is similar to that demonstrated with interpulse spectrometers, both by the Aerodyne group<sup>17,27</sup> and very recently by the Rice University group.<sup>28</sup> In the latter study Wiedmann *et al.*<sup>28</sup> showed that, using a 100-m

path length, 50-Torr total pressure, a 10-kHz pulse repetition rate, and an 80-s acquisition time, a 100-ppb ethylene could be detected. Although our demonstrated sensitivity for ethylene was  $\sim 1.5$  ppm, we used a 5-Hz repetition frequency, a 1-s integration time, and a 66-m path length. As we have demonstrated with nitrous oxide, increasing the path length to 110 m, the repetition frequency to 20 kHz, and the integration time to 3.2 s, the sensitivity for ethylene detection with our method may be increased by a factor of approximately 6, giving a projected detection limit with 3.2-s averaging of 250 ppb.

The main limitation at present is the availability of lasers to cover appropriate regions, for example, both the 10- and 8- $\mu\text{m}$  lasers that we used were not optimized for detection of trace gases. However, in the future with recent advancements in QC-laser technology the wavelength region probed should be able to be customized to whatever gases are of interest, which would allow many other trace exhaust gases to be detected at similar sensitivities.

The authors thank the United Kingdom Engineering and Physical Sciences Research Council (EPSRC) for funding the initial part of this work through research grant GST/M69111 1999, and National Environmental Research Council (NERC) for funding the main part through research grant NER/T/S/2002/000052. M. T. McCulloch is grateful for the award of an EPSRC Research Studentship.

The authors thank A. D. R. Phelps, D. J. S. Birch, and R. Abrams for the loan of vehicles during these experiments. Finally we thank the following staff of the Environmental Molecular Science Laboratory at Pacific Northwest National Laboratory for supplying high-resolution Fourier-transform spectra of ethylene: T. A. Blake, S. W. Sharpe, and R. L. Sams.

#### References

1. A. Fried, B. P. Wert, B. Henry, and J. R. Drummond, "Airborne tunable diode laser measurements of formaldehyde," *Spectrochim. Acta Part A* **55**, 2097–2110 (1999).
2. D. Richter, A. Fried, B. P. Wert, J. G. Walega, and F. K. Tittel, "Development of a tunable mid-IR difference frequency laser source for highly sensitive airborne trace gas detection," *Appl. Phys. B* **75**, 281–288 (2002).
3. M. Nagele and M. W. Sigrist, "Mobile laser spectrometer with novel resonant multipass photoacoustic cell for trace-gas sensing," *Appl. Phys. B* **70**, 895–901 (2000).
4. A. A. Kosterev and F. K. Tittel, "Chemical sensors based on quantum cascade lasers," *IEEE J. Quantum Electron.* **38**, 582–591 (2002).
5. D. A. Yarekha, M. Beck, S. Blaser, T. Aellen, E. Gini, D. Hofstetter, and J. Faist, *Electron. Lett.* **39**, 1123–1125 (2003).
6. S. Anders, W. Schrenk, C. Pflugl, E. Gornik, G. Strasser, C. Becker, and C. Sirtori, "Room-temperature operation of Ga-As-based quantum cascade lasers processed as ridge and microcavity waveguides," *IEEE Proc. Optoelectron.* **150**, 282–283 (2003).
7. J. S. Yu, S. Slivken, L. Doris, and M. Razeghi, "High-power continuous-wave operation of a 6- $\mu\text{m}$  quantum cascade laser at room temperature," *Appl. Phys. Lett.* **83**, 2503–2505 (2003).
8. C. R. Webster, G. J. Flesch, D. C. Scott, J. E. Swanson, R. D. May, W. S. Woodward, C. Gmachl, F. Capasso, D. L. Sivco, J. N. Baillargeon, A. L. Hutchinson, and A. Y. Cho, "Quantum-

- cascade laser measurements of stratospheric methane and nitrous oxide," *Appl. Opt.* **40**, 321–326 (2001).
9. K. Namjou, S. Cai, E. A. Whittaker, J. Faist, C. Gmachl, F. Capasso, D. L. Sivco, and A. Y. Cho, "Sensitive absorption spectroscopy with a room-temperature distributed-feedback quantum cascade laser," *Opt. Lett.* **23**, 219–221 (1998).
  10. E. Normand, M. McCulloch, G. Duxbury, and N. Langford, "Fast, real-time spectrometer based on a pulsed quantum cascade laser," *Opt. Lett.* **28**, 16–18 (2003).
  11. M. T. McCulloch, E. L. Normand, N. Langford, G. Duxbury, and D. A. Newnham, "Highly sensitive detection of trace gases using the time-resolved frequency downchirp from pulsed quantum cascade lasers," *Opt. Soc. Am. B* **8**, 1761–1768 (2003).
  12. G. Baumbach, *Air Quality Control* (Springer-Verlag, Berlin, 1996), Chap. 2.1.6.
  13. R. G. Derwent, M. E. Jenkin, and S. M. Saunders, "Photochemical ozone creation potentials for a large number of reactive hydrocarbons under European conditions," *Atmos. Environ.* **30**, 181–199 (1996).
  14. G. Baumbach, *Air Quality Control* (Springer-Verlag, Berlin, 1996), Chap. 7.3.3.
  15. J. Kaspar, P. Fornasiero, and N. Hickey, "Automotive catalytic converters: current status and some perspectives," *Catal. Today* **77**, 419–449 (2003).
  16. J. B. McManus, P. L. Kebabian, and M. S. Zahniser, "Astigmatic mirror multipass absorption cells for long-path-length spectroscopy," *Appl. Opt.* **34**, 3336–3348 (1995).
  17. Q. Shi, D. D. Nelson, J. B. McManus, M. S. Zahniser, M. E. Parrish, R. E. Baren, K. H. Shafer, and C. N. Harward, "Quantum cascade infrared laser spectroscopy for real-time cigarette smoke analysis," *Anal. Chem.* **75**, 5180–5190 (2003).
  18. T. Beyer, M. Braun, S. Hartwig, and A. Lambrecht, "Linewidth measurements of free-running, pulsed, distributed-feedback quantum cascade lasers," *J. Appl. Phys.* **95**, 4551–4554 (2004).
  19. T. A. Blake, S. W. Sharpe, and R. L. Sams, Environmental Molecular Science Laboratory, Pacific Northwest National Laboratory, P.O. Box 999, Richland, Washington 99352 (personal communication, 2003).
  20. R. R. Ernst, "Sensitivity enhancement in magnetic resonance," in *Advances in Magnetic Resonance, Vol. II*, J. S. Waugh, ed. (Academic, New York, 1966), pp. 1–135.
  21. M. T. McCulloch, N. Langford, and G. Duxbury, "Observation of rapid passage induced saturation in the 10.25  $\mu\text{m}$  spectrum of ethylene using a frequency chirped quantum cascade laser," *Mol. Phys.*, submitted for publication.
  22. E. C. Richard, K. K. Kelly, R. H. Winkler, R. Wilson, T. L. Thompson, R. J. McLauchlin, A. L. Schmeltekopf, and A. F. Tuck, "A fast-response near-infrared tunable diode laser absorption spectrometer for *in situ* measurements of  $\text{CH}_4$  in the upper troposphere and lower stratosphere," *Appl. Phys. B* **75**, 183–194 (2002).
  23. L. S. Rothman, C. P. Rinsland, A. Goldman, S. T. Massie, D. P. Edwards, J.-M. Flaud, A. Perrin, C. Camy-Peyret, V. Dana, J.-Y. Mandin, J. Schroeder, A. McCann, R. R. Gamache, R. B. Wattson, K. Yoshino, K. V. Chance, K. W. Jucks, L. R. Brown, V. Nemtchinov, and P. Varanasi, "The HITRAN molecular database; 1996 edition," *J. Quant. Spectrosc. Radiat. Transfer* **60**, 665–710 (1998).
  24. W. E. Blass, J. J. Hillman, A. Fayt, S. J. Daunt, L. R. Senesac, A. C. Ewing, L. W. Jennings, J. S. Hager, S. L. Mahan, D. C. Reuter, and M. Sirota, "10- $\mu\text{m}$  ethylene: spectroscopy, intensities, and a planetary modeler's atlas," *J. Quant. Spectrosc. Radiat. Transfer* **71**, 47–60 (2001).
  25. A. G. Maki and J. S. Wells, "Wave-number calibration tables from heterodyne frequency measurements (version 1.3)," <http://physics.nist.gov/wavenu> (4 February 2003); originally published as NIST Spec. Publ. 821 (National Institute of Standards and Technology, Gaithersburg, Md., 1987).
  26. S. Schilt, L. Thevenaz, E. Courtois, and P. A. Robert, "Ethylene spectroscopy using a quasi-room-temperature quantum cascade laser," *Spectrochim. Acta Part A* **58**, 2533–2539 (2002).
  27. R. E. Baren, M. E. Parrish, K. H. Shafer, C. N. Harward, Q. Shi, D. D. Nelson, J. B. McManus, and M. S. Zahniser, "Quad quantum cascade infrared laser spectrometer with dual gas cells for the simultaneous analysis of mainstream and sidestream cigarette smoke," *Spectrochim. Acta Part A* **60**, 3437–3447 (2004).
  28. D. Wiedmann, A. A. Kosterev, C. Roller, R. F. Curl, M. P. Fraser, and F. K. Tittel, "Monitoring of ethylene by a pulsed quantum-cascade laser," *Appl. Opt.* **43**, 3329–3334 (2004).